This article was downloaded by: [University of Sydney]
On: 29 August 2013, At: 07:34
Publisher: Taylor & Francis
Informa Ltd Registered in England and Wales Registered Number: 1072954 Registered office: Mortimer House, 37-41 Mortimer Street, London W1T 3JH, UK

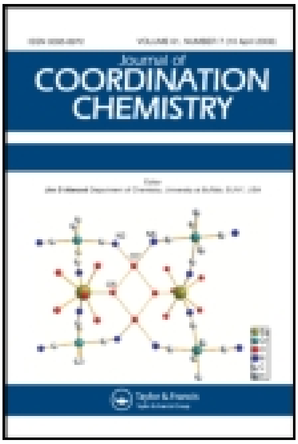

Journal of Coordination Chemistry
Publication details, including instructions for authors and subscription information:
http://www.tandfonline.com/loi/gcoo20

Decorating nickel phthalocyanine periphery by aryl-,,-oxadiazole pendants: synthesis, characterization, and conductivity studies

M.N.K. Harish [a] , J. Keshavayya [a] [a] , K.R. Venugopala Reddy [b] , H.R. Mallikarjuna [c] , R.A. Shoukat Ali [a] & T. Rajesh [a]

[a] Department of Chemistry, School of Chemical Sciences, Jnana Sahyadri, Kuvempu University, Shankaraghatta - 577 451, Shimoga, Karnataka, India

[b] Department of Industrial Chemistry, School of Chemical Sciences, Jnana Sahyadri, Kuvempu University, Shankaraghatta - 577 451, Shimoga, Karnataka, India

[c] Department of Chemistry, Rajiv Institute of Technology, Hassan - 573 201, Karnataka, India

Published online: 20 Nov 2010.

To cite this article: M.N.K. Harish , J. Keshavayya , K.R. Venugopala Reddy , H.R. Mallikarjuna , R.A. Shoukat Ali & T. Rajesh (2010) Decorating nickel phthalocyanine periphery by aryl-,,-oxadiazole pendants: synthesis, characterization, and conductivity studies, Journal of Coordination Chemistry, 63:23, 4050-4060, DOI: 10.1080/00958972.2010.529902

To link to this article: http://dx.doi.org/10.1080/00958972.2010.529902

PLEASE SCROLL DOWN FOR ARTICLE

Taylor & Francis makes every effort to ensure the accuracy of all the information (the "Content") contained in the publications on our platform. However, Taylor & Francis, our agents, and our licensors make no representations or warranties whatsoever as to the accuracy, completeness, or suitability for any purpose of the Content. Any opinions and views expressed in this publication are the opinions and views of the authors, and are not the views of or endorsed by Taylor & Francis. The accuracy of the Content should not be relied upon and should be independently verified with primary sources of information. Taylor and Francis shall not be liable for any losses, actions, claims, proceedings, demands, costs, expenses, damages, and other liabilities whatsoever or howsoever caused arising directly or indirectly in connection with, in relation to or arising out of the use of the Content.

This article may be used for research, teaching, and private study purposes. Any substantial or systematic reproduction, redistribution, reselling, loan, sub-licensing, systematic supply, or distribution in any form to anyone is expressly forbidden. Terms & Conditions of access and use can be found at http://www.tandfonline.com/page/terms-and-conditions

Downloaded by [University of Sydney] at 07:34 29 August 2013

Journal of Coordination Chemistry
Vol. 63, No. 23, 10 December 2010, 4050–4060

Decorating nickel phthalocyanine periphery by aryl-[1,3,4]-oxadiazole pendants: synthesis, characterization, and conductivity studies

M.N.K. HARISH†, J. KESHAVAYYA*†, K.R. VENUGOPALA REDDY‡, H.R. MALLIKARJUNA§, R.A. SHOUKAT ALI† and T. RAJESH†

†Department of Chemistry, School of Chemical Sciences, Jnana Sahyadri, Kuvempu University, Shankaraghatta – 577 451, Shimoga, Karnataka, India
‡Department of Industrial Chemistry, School of Chemical Sciences, Jnana Sahyadri, Kuvempu University, Shankaraghatta – 577 451, Shimoga, Karnataka, India
§Department of Chemistry, Rajiv Institute of Technology, Hassan – 573 201, Karnataka, India

(*Received 24 June 2010; in final form 1 September 2010*)

We have decorated nickel phthalocyanine (NiPc) periphery by four different aryl-[1,3,4]-oxadiazole pendants. Introduction of aryl-[1,3,4]-oxadiazole pendants into the NiPc core results in improved thermal stability, fine-tuning of the position of the Q-band with decrease in band gap, indicating effective electronic communication between the two different ring systems with NiPc core. The magnitude of DC electrical conductivity for aryl-[1,3,4]-oxadiazole-substituted NiPcs **3a**–**3d** is found to be $\sim 10^5$ times higher than the parent NiPc (**1**). The temperature-dependent DC conductivity studies reveal semiconducting nature of the newly synthesized NiPc compounds with significant decrease in thermal activation energy (ΔE) compared to parent NiPc.

Keywords: Phthalocyanine; [1,3,4]-Oxadiazole; Conducting; Solid-state electronic absorption spectra; Solid-state ^{13}C-NMR

Downloaded by [University of Sydney] at 07:34 29 August 2013

1. Introduction

Peripheral functionalization of phthalocyanines (Pcs) and their metal Pcs (MPcs) complexes have attracted attention because of their electronic structures, extreme thermal, and chemical stabilities, giving rise to applications in materials science [1–4]. In addition to their intrinsic use as dyes and pigments, MPcs have demonstrated potential in emerging technologies including sensors [5], photovoltaic cell elements [6], photoconducting agents [7], nonlinear optics [8], liquid crystals [9], electrocatalysis, and fuel cells [10, 11]. Research in the recent years has focused on tuning the properties of related macrocycles *via* changes in their chemical structure.

In 1990, [1,3,4]-oxadiazole functionalized organic molecules were found to serve as excellent electron-transporting [12–16] and hole-blocking materials [17].

---

*Corresponding author. Email: jkeshavayya@gmail.com

Journal of Coordination Chemistry
ISSN 0095-8972 print/ISSN 1029-0389 online © 2010 Taylor & Francis
DOI: 10.1080/00958972.2010.529902

As planar organic semiconducting material, oxadiazole is an attractive building block for organic light emitting devices because of its electron affinity and ease in building a stable π-conjugated system [18, 19]. Introduction of an oxadiazole ring is a promising approach to attain high charge-carrier mobility, making them prime candidates for applications in organic electronics [20–22].

Thus, functionalization of Pc with oxadiazole and an aryl system is desirable. Prior to our study, there was only one report pertaining to the synthesis of Pc bearing [1,3,4]-oxadiazole moieties with phenyl ether linkage, with improved solubility and electrical conductivity [23]. This encouraged us to synthesize Pc macrocycles with aryl-1,3,4-oxadiazole subunits. This initial study to develop a new peripheral modified Pcs involves incorporation of heteroaromatic and aromatic moieties. The synthetic route in this study involves direct association of aryl oxadiazole pendants to Pc allowing extensive electronic interaction of Pc with oxadiazole and aryl substituent. Investigation on these new Pcs may be regarded as an important step in developing viable sensor and semiconducting materials with high chemical and thermal stabilities. Further, the synthetic scheme is very general and the possibilities are only highlighted by this preliminary study.

All the newly synthesized 2,9,16,23-tetra-aryl-[1,3,4]-oxadiazole-substituted nickel phthalocyanines (NiPcs) **3a**–**3d** are bottle green in color. Characterization of these Pc complexes was difficult because of insolubility in almost all organic solvents. Nevertheless, the elemental analysis, FT-IR, solid-state UV-Vis, and solid-state ^{13}C-NMR spectroscopy, in addition to X-ray diffraction (XRD), scanning electron microscopy (SEM, spectral and thermal analyses provided sufficient evidence for the proposed structures.

Downloaded by [University of Sydney] at 07:34 29 August 2013

2. Experimental

2.1. *Materials*

1,2,4-Benzene tricarboxylic anhydride was purchased from Aldrich and other chemicals were obtained from Merck (India) and used without purification. Tetracarboxy nickel phthalocyanine (TCPNi) [24] and aryl hydrazides **2a**–**2d** [25] were prepared according to the described procedure.

2.2. *Instrumentation*

Elemental analyses were obtained from a Carlo-Erba 1106 instrument. Infrared (IR) spectra were recorded on a FT-IR 8400s Shimadzu spectrometer in KBr pellets. Solid-state electronic absorption spectra were recorded on a Perkin-Elmer UV-Vis spectrometer, model UV/VIS-35. Solid-state ^{13}C-NMR spectra were recorded on a Bruker DSX-300 solid-state NMR spectrometer with a magnetic field of 7.04 T and carbon frequency of 75.47 MHz (internal standard was glycine). Powdered XRD measurements were carried out on a Bruker D8 Advance X-ray diffractrometer. DC electrical conductivity measurements were carried out by the two-probe method using a Keithley source meter (Model-2400). A calibrated Chromel–Alumel thermocouple was used to measure the temperature of the sample. For DC electrical conductivity measurements, powder samples were pressed uniaxially into a pellet of thickness ≈2 mm and of diameter 10 mm by applying a pressure of 100 Mpa for 3 min. The pellets were sintered at 100°C for 3 h to eliminate trapped oxygen and to get thermal stability. Fine quality silver paint was applied on both sides of the pellets for good electrical contacts. The pellet was sandwiched tightly between two steel rods in a sample holder with the help of screws and kept in a cell. Then, the cell was placed in a muffle furnace. A suitable constant and low voltage (5 V) was applied across the pellet and the corresponding current through the sample was measured from 300 to 500 K; conductivity readings were recorded during the heating cycle.

2.3. *General method for the synthesis of 2,9,16,23-tetra-aryl-[1,3,4]-oxadiazole-substituted NiPc*

TCPNi (0.001 mol) and aromatic hydrazide (**2a**–**2d**) (0.006 mol) were stirred into preheated polyphosphoric acid (PPA) (100 g) containing 10 g of P_2O_5 at 100°C in a three-necked round bottom flask containing a mechanical stirrer, condenser, and thermometer for 1 h and then maintained at 150°C for 20 h. The reaction mixture was allowed to cool to 100°C and quenched with ice cold water and filtered. The product obtained was repeatedly treated with 0.1N sodium hydroxide solution followed by water, hot acetic acid, 10% sodium bicarbonate solution, water, and acetone to get **3a**–**3d**.

2.3.1. 2,9,16,23-Tetra-{5-(phenyl)[1,3,4]-oxadiazole}-nickel phthalocyanine (3a). Yield: 80%. Calcd: C (66.97), H (2.81), N (19.53). Found: C (66.03), H (2.12), N (18.94). IR [(KBr) ν_{max}/cm^{-1}]: 3065 (Ar–CH), 2922 (Ar–CH), 2848 (Ar–CH), 1609 (C=N), 1530 (C=C), 1092, 930, 824, 724 (Pc skeleton vibration). ^{13}C-NMR (solid state) δ/ppm 217, 163, 150–120. UV-Vis (solid state) λ_{max}/nm 497, 602, 666, 768.

2.3.2. 2,9,16,23-Tetra-{5-(4-methyl-phenyl)[1,3,4]-oxadiazole}-nickel phthalocyanine (3b). Yield: 82%. Calcd: C (67.84), H (3.35), N (18.62). Found: C (67.61), H (2.98), N (18.13). IR [(KBr) ν_{max}/cm^{-1}]: 3067 (Ar–CH), 2919 (Ar–CH), 2854 (Ar–CH), 1609 (C=N), 1528 (C=C), 1138, 1089, 920, 829, 727 cm^{-1} (Pc skeleton vibration). ^{13}C-NMR (solid state) δ/ppm 219, 162, 150–120, 20. UV-Vis (solid state) λ_{max}/nm 484, 603, 667, 785.

2.3.3. 2,9,16,23-Tetra-{5-(4-chloro-phenyl)[1,3,4]-oxadiazole}-nickel phthalocyanine (3c). Yield: 86%. Calcd: C (59.80), H (2.20), N (17.43). Found: C (59.73), H (2.03), N (17.04). IR [(KBr) ν_{max}/cm^{-1}]: 3067 (Ar–CH), 2923 (Ar–CH), 2848 (Ar–CH), 1603 (C=N), 1530 (C=C), 1092, 926, 837, 734 (Pc skeleton vibration). ^{13}C-NMR (solid state) δ/ppm 213, 162, 150–120. UV-Vis (solid state) λ_{max}/nm 482, 604, 668, 784.

2.3.4. 2,9,16,23-Tetra-{5-(4-nitro-phenyl)[1,3,4]-oxadiazole}-nickel phthalocyanine (3d). Yield: 80%. Calcd: C (57.89), H (2.13), N (21.10). Found C (57.8), H (1.97), N (20.04). IR [(KBr) ν_{max}/cm^{-1}]: 3067 (Ar–CH), 2923 (Ar–CH), 2854 (Ar–CH), 1606 (C=N), 1523

Downloaded by [University of Sydney] at 07:34 29 August 2013

(C=C), 1338, 1094, 926, 851, 725 (Pc skeleton vibration). ^{13}C-NMR (solid state) δ/ppm 223, 162, 150–120. UV-Vis (solid state) λ_{max}/nm 481, 603, 667, 787.

3. Results and discussion

3.1. *Synthesis*

The target 2,9,16,23-tetraaryl 1,3,4-oxadiazole-substituted NiPcs (**3a**–**3d**) were obtained in good yield through the melt condensation of TCPNi with four different aromatic hydrazides **2a**–**2d** in the presence of PPA as a solvent and condensing agent (scheme 1). A similar reaction employing $POCl_3$ for cyclization resulted in very poor yield (<28%).

3.2. *IR absorption spectra*

FT-IR spectra for **3a**–**3d** exhibited a series of absorptions at 725–735, 840–851, 920–926, 1089–1094, and 1142–1138 cm^{-1}, attributed to the Pc skeleton. Peaks at 1603–1614 and 1528–1530 cm^{-1} for **3a**–**3d** can be assigned to aromatic –C=N– and –C=C– in plane skeletal vibrations of the Pc core. Peaks at 3030–3070 and 2930–2850 cm^{-1} are associated with aromatic –C–H stretching vibrations; a peak in the region 1088–1095 cm^{-1} is due to aromatic –C–H bending vibrations. Comparison of FT-IR spectra of TCPNi and **3a**–**3d** reveals some marked differences; the characteristic intense absorption due to –C=O (–COOH) of TCPNi at 1697 cm^{-1} disappear in IR spectra of **3a**–**3d**, indicating involvement of carboxy in condensation followed by cyclization with acid hydrazides. The characteristic stretching vibrations due to –C=N– and –C–O– of the oxadiazole ring in **3a**–**3d** is coupled to skeletal vibrational peaks of –C=N– and –C=C– of the Pc core. Emergence of two intense bands at 1523 and 1338 cm^{-1} for **3d** was assigned for NO_2

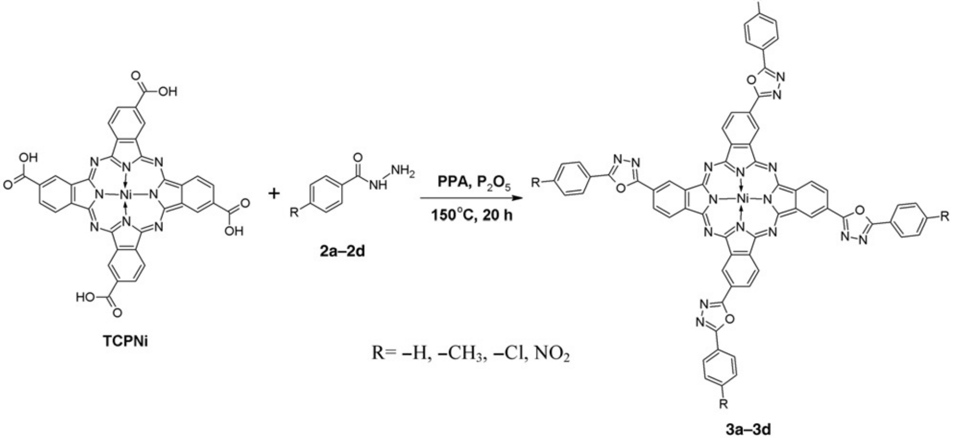

Scheme 1. Synthesis of tetraaryl-[1,3,4]-oxadiazole-substituted NiPc.

Downloaded by [University of Sydney] at 07:34 29 August 2013

asymmetric and symmetric stretches, respectively. Characteristic –CH_3 and –C–Cl functionality in **3b** and **3d** is shown by peaks at 2919 and 514 cm^{-1}, respectively.

3.3. *Solid-state ^{13}C-NMR spectra*

Solid-state ^{13}C-NMR spectra of **3a**–**3d** exhibit the expected broad signal at 120–150 ppm and an additional peak at 162–165 ppm for aromatic carbons and aromatic carbons attached to nitrogen, respectively. Peaks at 213–221 ppm were assigned to carbons attached to the electron deficient oxadiazole in **3a**–**3d**. A peak at 20 ppm confirms the presence of –CH_3 in 3**b** (Supplementary material).

3.4. *Electronic absorption spectra*

Marked difference is apparent in representative solid-state electronic absorption spectra of unsubstituted NiPc and **3a**–**3d** (figure 1) and results are summarized in table 1.

Electronic spectra recorded from **3a**–**3d** in solid state exhibit characteristic Q-band in the region $\lambda \approx 600$ nm and a second band of lower intensity in near-IR region at $\lambda \approx 780$ nm. The electron-acceptor oxadiazole pendants induced redshift and splitting of

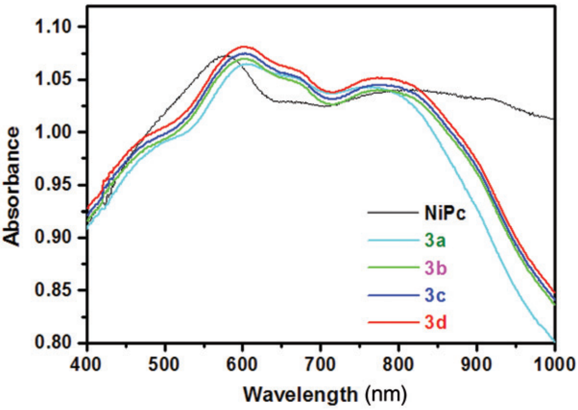

Figure 1. Solid-state electronic absorption spectra for NiPc and **3a**–**3d**.

Table 1. Solid-state electronic absorption data for NiPc (**1**) and **3a**–**3d**.

NiPc	Peaks λ_{max} (nm)
1	577
3a	497, 602, 666, 768
3b	484, 603, 667, 785
3c	482, 604, 668, 784
3d	481, 603, 667, 787

Downloaded by [University of Sydney] at 07:34 29 August 2013

Table 2. Optical band gap data for NiPc (**1**) and **3a**–**3d**.

NiPc	Peaks λ_{max} (nm)	Band gap (eV)
1	577	2.04
3a	602	1.974
	768	1.461
3b	603	1.974
	785	1.444
3c	604	1.974
	784	1.446
3d	603	1.974
	787	1.461

the Q-band due to a_{2u}-to-e_g and b_{2u}-to-e_g transitions, indicating effective electronic communication between the two different ring systems of the Pc core [26, 27].

Optical band gaps for **3a**–**3d** were determined by the absorption edge of the absorption spectrum of each compound in the solid state, and the data are summarized in table 2.

Since interactions of MPc molecules are of van der Waals type, rearrangements of molecule alter the energy band gap between valence and conduction bands. A decrease in optical band gap for NiPcs **3a**–**3d** is observed by the introduction of aryl oxadiazole pendants to the NiPc periphery as compared to NiPc. In **3a**–**3d**, the Ni is in a position of nearest approach to nitrogens in parallel molecules, and the presence of heteroaromatic oxadiazole and phenyl rings in the Pc periphery results in extended conjugation and increased orbital overlap between parallel pairs of molecules influence the stacking arrangements and crystal phase of the Pc molecules [1, 2, 28, 29].

3.5. *Scanning electron microscopy*

Morphology of the synthesized NiPcs was studied by SEM analysis. The particulates of **3a**–**3d** are not uniform in shape (figure 2); the diameter of particulates was in the range 400–5000 nm. NiPc attached to the aryl oxadiazole pendant can act as a nucleation center, which further induces growth of Pc crystallite. Since the aryl oxadiazole pendants were distributed along the periphery of the NiPc core, the size of crystallite was restricted by the accessibility of adjacent Pc molecules. On the contrary, aggregation of oxadiazole-substituted NiPc can hardly be prevented.

3.6. *Thermal analysis*

Analysis of TG curves of **3a**–**3d** indicate three-step decomposition. The first step at 30–105°C may be accounted for by loss of water. The second degradation at 200–450°C can be accounted for by loss of peripheral phenyl. The third step from 400 to 900°C may be due to the Pc core [30].

Downloaded by [University of Sydney] at 07:34 29 August 2013

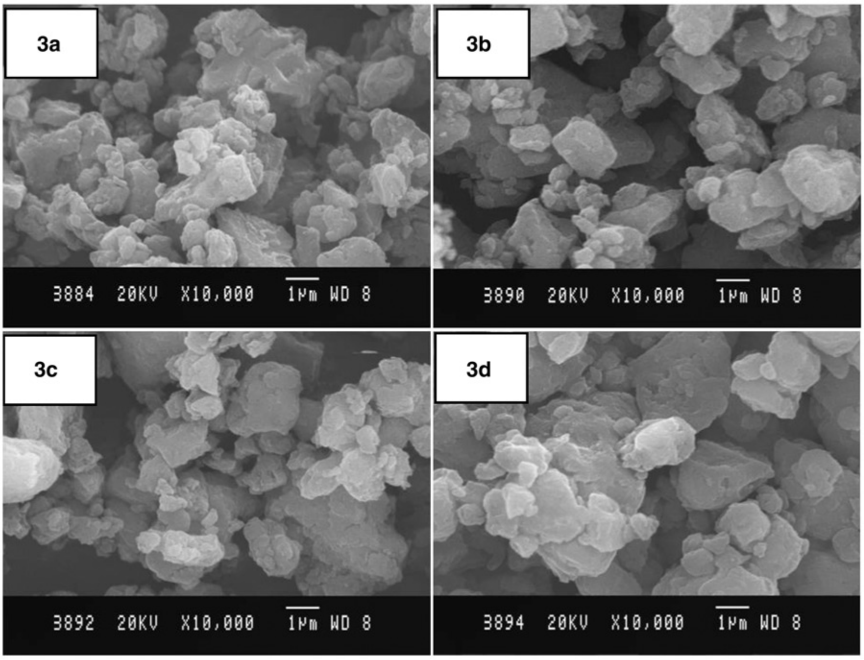

Figure 2. SEM micrographs for **3a**–**3d**.

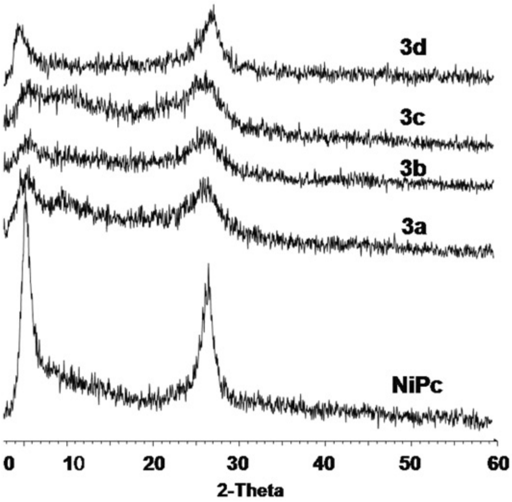

Figure 3. Powder XRD patterns for NiPc and **3a**–**3d**.

3.7. *XRD studies*

The powdered XRD pattern of NiPc and **3a**–**3d** are shown in figure 3. The diffraction pattern of the oxadiazole-substituted Pc exhibited characteristic broad peaks.

Downloaded by [University of Sydney] at 07:34 29 August 2013

Table 3. Powdered XRD data for NiPc (**1**) and **3a**–**3d**.

NiPc	2θ (degrees)	Lattice spacing (d) (Å)	Relative intensity
1	5.70	15.4860	100
	27.01	3.2975	74.3
3a	26.23	3.1427	100
	5.76	15.3036	98.7
	6.53	13.5151	86.7
	7.87	11.495	75.4
3b	25.20	3.4902	100
	5.10	17.3135	73.8
	6.00	14.7060	93.8
	7.62	11.5925	76.4
3c	26.48	3.3626	100
	5.16	17.1024	89.1
	6.91	12.7669	88
	7.34	12.0285	86.8
3d	27.38	3.2538	100
	5.15	17.1315	79
	6.32	13.9668	56.9
	7.34	12.0221	49.6

The heteroaromatic oxadiazole and phenyl rings in the Pc result in extended conjugation and the greater π-electron region influences the stacking of the Pcs in parallel molecules. The interplanar distances for **3a**–**3d** are less than the parent NiPc, due to the aryl oxadiazole pendants. Data (2θ, lattice spacing, and relative intensity) are provided in table 3.

3.8. *DC electrical conductivity studies*

The values of room temperature DC electrical conductivity observed for **3a**–**3d** are $\sim 10^5$ times higher than the parent NiPc [31], in the order **3d** > **3c** > **3b** > **3a**.

Increase in conductivity for **3a**–**3d** can be attributed to substitution at the Pc periphery, resulting in extended conjugation. The oxadiazole as an electron-deficient ring system can act as a π-electron acceptor. The presence of 12 heteroatoms in the Pc periphery influences the stacking of the Pc molecules increasing the orbital overlap between parallel pairs of molecules. This results in decrease in the intersegment spacing and provides a pathway for charge carriers.

The temperature dependence of conductivity can be expressed as

$$\sigma = \sigma_0 \exp\left[\frac{-\Delta E}{kT}\right],$$

where σ is the DC electrical conductivity at temperature T, σ_0 is the pre-exponential factor, k is Boltzmann's constant, and ΔE is the activation energy.

Figure 4(a) shows variation of resistivity with temperature. For **3a**–**3d**, the resistivity decreases with increase in temperature. Further, figure 4(b) represents the Arrhenius

Downloaded by [University of Sydney] at 07:34 29 August 2013

Downloaded by [University of Sydney] at 07:34 29 August 2013

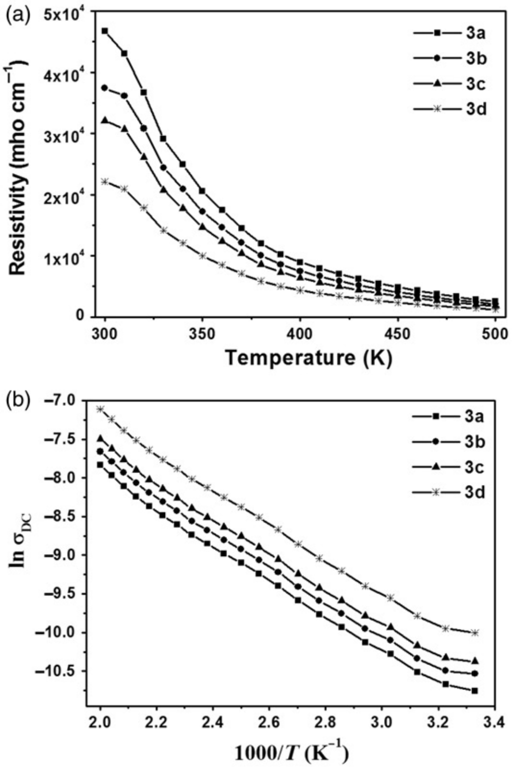

Figure 4. (a) Variation of resistivity with temperature for **3a**–**3d** and (b) Arrhenius plots for **3a**–**3d**.

Table 4. Activation energies for **3a**–**3d**.

NiPc	Conductivity σ_{DC} at 300 K (mho cm^{-1})	ΔE (300–500 K) (eV)
3a	2.14046×10^{-5}	0.108
3b	2.67069×10^{-5}	0.105
3c	3.11583×10^{-5}	0.102
3d	4.52733×10^{-5}	0.101

plots of $\log \sigma_{DC}$ (DC conductivity) *versus* $1/T$ (reciprocal of temperature) for **3a**–**3d** from 300 to 500 K. The thermal activation energies (ΔE) obtained from Arrhenius plots are shown in table 4; ΔE for **3a**–**3d** is considerably less than the parent NiPc [31]. The plots reveal that temperature has pronounced effect on DC conductivity. All the newly synthesized Pc molecules are semiconducting in nature. The increase in DC electrical conductivity of **3a**–**3d** with increase in temperature can be explained for conduction occurs by electron transfer across insulating gaps in the conducting pathway by fluctuation-induced tunneling model, proposed by Sheng [32] and hopping at the localized states in the amorphous regions between the small metallic regions [33].

4. Conclusion

We have shown that NiPc decorated with aryl-[1,3,4]-oxadiazole pendants, **3a**–**3d**, exhibit improved thermal stability and could absorb visible light from 400 to 800 nm. The presence of electron-acceptor oxadiazole pendants resulted in fine-tuning of the position of the Q-band with decreased optical band gap. The room temperature DC electrical conductivity for **3a**–**3d** is $\sim 10^5$ times higher than the parent NiPc and it increases with increase in temperature with significant decrease in thermal activation energy (ΔE). This study has revealed that these new Pcs can serve as an excellent optical, sensor, and charge-carrier semiconducting materials with high chemical and thermal stabilities [34]. Further, investigation on electrocatalytic properties of aryl-[1,3,4]-oxadiazole-substituted NiPcs is in progress.

Downloaded by [University of Sydney] at 07:34 29 August 2013

Acknowledgments

The authors thank Prof. S. Natrajan, IISc, Bangalore for providing solid-state electronic absorption spectra, as well as NMR Research Center, IISc, Bangalore for providing solid-state ^{13}C-NMR spectra.

References

[1] C.C. Leznoff, A.B.P. Lever. *Phthalocyanines: Properties and Applications*, Vols I–IV, VCH Publications Inc., New York (1986–1993).
[2] N.B. McKeown. *Phthalocyanine Materials – Synthesis Structure and Function*, Cambridge University Press, Cambridge (1998).
[3] K. Kadish, K.M. Smith, R. Guilard. *The Porphyrin Handbook*, Vols 15–20, Academic Press, New York (2003).
[4] H.S. Nalwa. *Supramolecular Photosensitive and Electroactive Materials*, Academic Press, New York (2001).
[5] O.A. Osmanbas, A. Koca, I. Ozcesmeci, A.I. Okur, A. Gul. *Electrochim. Acta*, **53**, 4969 (2008).
[6] J. Yum, S. Jang, R. Humphry-Baker, M. Gratzel, J. Cid, T. Torres, Md.K. Nazeeruddin. *Langmuir*, **24**, 5636 (2008).
[7] A. Schuetze, N. Pieper, J. Zacheja. *Sens. Actuators B*, **B23**, 215 (1995).
[8] G. de la Torre, P. Vazquez, F. Agullo-Lopez, T. Torres. *Chem. Rev.*, **104**, 3723 (2004).
[9] B.A. Minch, W. Xia, C.L. Donley, R.M. Hernandez, C. Carter, M.D. Carducci, A. Dawson, D.F. O'Brien, N.R. Armstrong. *Chem. Mater.*, **17**, 1618 (2005).
[10] F. Harnisch, N.A. Savastenko, F. Zhao, H. Steffen, V. Bruser, U. Schroder. *J. Power Sources*, **193**, 86 (2009).
[11] R. Baker, D.P. Wilkinson, J. Zhang. *Electrochim. Acta*, **54**, 3098 (2009).
[12] C. Adachi, T. Tsutsui, S. Saito. *Appl. Phys. Lett.*, **56**, 799 (1990).
[13] C. Adachi, T. Tsutsui, S. Saito. *Appl. Phys. Lett.*, **57**, 531 (1990).
[14] C. Risko, E. Zojer, P. Brocorens, S.R. Marder, J.L. Bredas. *Chem. Phys.*, **313**, 151 (2005).
[15] S. Janietz, S. Anlauf, A. Wedel. *Macromol. Chem. Phys.*, **203**, 433 (2002).
[16] X. Zhan, Y. Liu, X. Wu, S. Wang, D. Zhu. *Macromolecules*, **35**, 2529 (2002).
[17] P. Zhao, X. Zhu, J. Chen, D. Ma, W. Huang. *Synth. Met.*, **156**, 763 (2006).

[18] N.A. Zafiropoulos, E. Choi, T. Dingemans, W. Lin, E.T. Samulski. *Chem. Mater.*, **20**, 3821 (2008).

[19] A. Carella, A. Castaldo, R. Centore, A. Fort, A. Sirigu, A. Tuzi. *J. Chem. Soc., Perkin Trans.*, **2**, 1791 (2002).

[20] L. Chen, C. Yang, M. Li, J. Qin, J. Gao, H. You, D. Ma. *Cryst. Growth Des.*, **7**, 39 (2007).

[21] H.K. Christian-Pandya, Z.I. Niazimbetova, F.L. Beyer, M.E. Galvin. *Chem. Mater.*, **19**, 993 (2007).

[22] C.C. Chiang, H. Chen, C. Lee, M. Leung, K. Lin, K. Hsieh. *Chem. Mater.*, **20**, 540 (2008).

[23] S. Chen, Y. Liu, Y. Xu, Y. Sun, W. Qiu, X. Sun, D. Zhu. *Synth. Met.*, **156**, 1236 (2006).

[24] X. Song, Y. She, H. Ji, Y. Zhang. *Org. Process Res. Dev.*, **9**, 297 (2005).

[25] B. Furniss, A.H. Hannaford, P.W.G. Smith, A.R. Tatchell. *Vogel's Textbook of Practical Organic Chemistry*, 5th Edn, p. 1077, Addison Wesley Longman, New Delhi (1998).

[26] H. Kantekin, M. Rakap, M.N. Misir, H.Z. Gok, I. Acar. *J. Coord. Chem.*, **60**, 1965 (2007).

[27] H. Kantekin, Y. Gok, M.B. Kilicaslan, I. Acar. *J. Coord. Chem.*, **61**, 229 (2009).

[28] M. Ichikawa, T. Kawaguchi, K. Kobayashi, T. Miki, K. Furukawa, T. Koyama, Y. Taniguchi. *J. Mater. Chem.*, **16**, 221 (2006).

[29] D.M.P. Mingos (series Ed.), J. Jiang (volume Ed.). *Structure and Bonding*: *Functional Phthalocyanine Molecular Materials,* Springer-Verlag, Berlin, Heidelberg (2010). DOI 10.1007/978-3-642-04752-7_1.

[30] A. Broido. *J. Polym Sci., Part A-2: Polym. Phys.*, **7**, 1761 (1969).

[31] M.M. El-Nahass, A.F. El-Deeb, F. Abd-El-Salam. *Org. Electron.*, **7**, 261 (2006).

[32] P. Sheng. *Phys. Rev. B*, **21**, 2180 (1980).

[33] Y.J. Wang, M.D. Newton, J.W. Davenport. *Phys. Rev. B*, **46**, 11935 (1992).

[34] H. Shiokawa, M. Hiramoto. *Mol. Cryst. Liq. Cryst.*, **491**, 277 (2008).

Downloaded by [University of Sydney] at 07:34 29 August 2013